International Journal of Sustainable and Green Energy
2025, Vol. 14, No. 1, pp. 20-31
https://doi.org/10.11648/j.ijsge.20251401.12

Research Article

Experimental and Numerical CFD Analysis of a Solar Dryer with Integration of Basalt Thermal Bed for Heat Storage

Serigne Thiao[1, *], Omar Drame[3], Awa Mar[2], Lat Grand Ndiaye[1], Issakha Youm[4]

[1]Laboratory of Chemistry and Physics of Materials (LCPM)/Department of Physics, Assane Seck Universty of Ziguinchor, Ziguinchor, Senegal

[2]Pole of Sciences and Technologies, Higher School of Engineering Sciences and Techniques, Amadou Moktar MBOW University of Dakar (UAM), Dakar, Senegal

[3]Thermo-Hydrodynamic Instabilities Research Group of the Fluid Mechanics and Applications Laboratory (MFA)/Department of Physics, Cheikh Anta Diop University of Dakar, Dakar, Senegal

[4]Laboratory of Solar Energy, Materials and Systems/Departement of Physics, Cheikh Anta DIOP University, Dakar, Senegal

Abstract

Solar thermal energy is available in abundance in a country like Senegal where direct solar radiation is on average 1950kWh/m^2 per year. Solar drying is the most popular method to preserve food in our country. However, it is limited by the intermittent nature of the sun. The objective of this paper is to overcome the intermittency of the sun by integrating a thermal bed into the solar dryer. The thermal bed is made of basalt and biochar for heat storage and humidity absorption respectively. An experimental study was done using papaya and moringa leaves. The results obtained show that the thermal bed stores heat at the temperature of 39 ℃ at 10p.m. Papaya is dried in two days and moringa leaves are dried in one day. For papaya slices, water content is 15% and was reached at the second day of drying. Also, moringa dry leaves water content is 8%. This value begins to be reached from 3 p.m. in the afternoon. Thus, the thermal bed temperature, the air temperature between the drying racks and the drying chamber outlet air temperature are respectively an average of 48.67 ℃, 48 ℃ and 47.22 ℃ compared to 34.33 ℃ of the ambient temperature, a difference of more than 4 ℃. The experimental study is supported by a Computational fluid dynamic (CFD) analysis.

Keywords

Basalt, CFD, Dryer, Direct Solar Radiation, Heat Storage, Solar Thermal Energy, Thermal Bed

1. Introduction

In the majority of our countries, agriculture represents the biggest part of economic activity. Most of 80% in working population is in agriculture sector. Despite these large numbers in agriculture sector, there are still food problems in the world. Also, the global population is predicted to exceed eight billion by the year 2025 [1]. Food production must therefore be in-

*Corresponding author: Serignethiao12@yahoo.fr (Serigne Thiao)

Received: 16 October 2024; **Accepted:** 6 November 2024; **Published:** 10 February 2025

creased to meet the growing global demand for food [2]. Significant losses after many harvests are due to a lack of storage means. These losses have negative effects on production yields [3]. Waste of agri-food products must also be avoided for good food safety [4, 5]. Fruits and vegetables can be preserved effectively by the drying technique [6]. Drying is one of the first unit operations farmers perform in the chain of processing steps to either extend the shelf life of their products for storage or prepare them for secondary processing [7]. The drying process is based on energy and mass balances [8]. Solar thermal energy can offer desirable energy for several purposes, such as industrial, domestic, and agri-food conservation [9]. Solar drying offers many benefits for agricultural producers and consumers. It is a viable and sustainable method of processing that adds value to agriculture and contributes to its development [10]. The solar drying included direct drying by a greenhouse (DD), indirect solar dryer operating in continuous (IC) and discontinuous (ID) modes, and all were compared to those obtained by lyophilization (control) [11]. A three-stage convection solar dryer was developed and evaluated by M. Usama et al., [12]. Their study is interesting. It can help to improve performance of solar thermal drying methods for temperature control and energy efficiency. One notable advantage of utilizing a passive solar dryer is its reliance on natural energy sources, such as solar heat and radiation [13]. R. J. Mongi [14] examines the physicochemical properties and shelf life of mango and pineapple dried by solar energy. The conception of a storage system makes it possible to balance demand and availability [15]. Thermal energy storage (TES) technologies have proven to be effective in storing surplus energy and delivering it when renewable sources cannot meet the demand. Energy storage is proposed to provide a stable and reliable energy supply, reducing fluctuations in output power for renewable technologies [16]. Solar energy and storage technologies are helping to combat current global climate change [17]. Research into heat storage techniques in dryer's solar system can increase the reliability of solar energy for drying. [8]. Thermal energy storage integration system with solar air heater holds an immense potential for optimizing the energy management in drying application [18]. Thermal energy storage (TES) provides several opportunities for efficient energy use and conservation. J. Ellis et al., [19] used, in their experimental work, flake salt as a storage medium. Therefore, their results showed that the moisture content is reduced from 30% to 11% in 6 hours. However, we note that the moisture content could only be reduced from 30% to 13% in 24 hours without the presence of the storage system. The temperature at the storage system was found to be between 110 ℃ and 72.2 ℃. Phase change materials show great promise as a potential thermal energy storage medium [20]. Much research shows that, molten salts, specifically the eutectic mixture of 60:40 $NaNO_3$-KNO_3, so-called solar salts, stand as the predominant choice for TES in CSP plants [21, 23, 24]. Solar molten salts, with a mixture of 60% $NaNO_3$ and 40% KNO_3, have been used as thermal energy storage medium in concentrating solar power plants [21]. Serigne, T et al., [22] use in their study a thermal bed made in basal as a thermal energy stotage. The result obtained shows that between 10:00 a.m. and 2:00 p.m., temperature variations were noted at the level of the thermal bed, the air between the racks and the air at the outlet of the drying chamber, respectively an average of 40 ℃, 39, 33 ℃ and 37.89 ℃. The optimal configuration for latent heat storage applied to solar heat for industrial processes was carried by M. Barnetche et al., [25]. Latent heat storage has the potential to store 4 times more energy than conventional sensible storage, making it particularly interesting for industrial applications with a lack of space. Barium Hydroxide Octahydrate [$Ba(OH)_2$. $8H_2O$] was used as PCM which can store the energy in the daytime and release it during off-sunshine hours [26]. Their system saved 5604 kWh of electrical energy and 555.06 liters of diesel fuel each year, as well as reduced 5.49 t CO_2 emissions. According to Y. Muhammad et al., [27], Several types of thermal storages are in the market. Other types are in research and development phases such as sensible thermal energy storage. M.C. Gilago, V.R. Mugi and C. V.P., [28] have carried out the drying kinetics of carrots and the efficiency of an indirect solar dryer without and with thermal energy storage. D. Tadele Embiale and D. Gudeta Gunjo [29] carried out a solar drying system with double pass solar air heater coupled with paraffin wax based latent heat storage. Their study is focused on the storage materials. H.U. Rehman et al., [30] carried out an experimental study on solar dryer with integrated thermal storage chamber. Forced convection indirect solar drying system that has a DPSAH, shell and tube type latent heat storage with paraffin as phase change material (PCM), blower and drying chamber is developed and tested by D. Tadele Embiale and D. Gudeta Gunjo [29]. A numerical study is conducted on the DPSAH to determine effect of mass flow on its performance and appropriate flow rate is selected for the drying experiment. Majeed, A. H., et al., [31] elucidate in their study the evaluation of performance for an indirect solar dryer, augmented with Phase Change Materials for food dehydration. Also Jaworski, M., et al., [32] carried out an experimental study of a phase change material for heat storage in a dryer. Thus, thinner tubes for heat transfer fluid are used. An indirect solar dryer intended for drying bananas and simulated under Ansys was developed byThaker, A.S., et al., [33]. Computational Fluid Dynamic can be used to carried out the performance of a novel research development in food dryer system [34]. Latent heat storage material integrated in solar dryer system is modeled using CFD by P. Lad et al., [35]. The model is reliable and can be employed to predict drying days of various food products when incorporated with PCM. S.E.D. Fertahi et al., [36] carried out CFD investigation of fine design influence of material phase change for heat storage. Petros Demissie et al., [37] carried out using CFD to model and simulate a cabinet type indirect solar dryer system. The aim of their study is to present as a tool for predicting flow and temperature distribution. Performance analysis of a small solar dryer equipped by storage materials for food conservation is

carried out by S. Rakshamuthu et al., [38]. In this study, the comparison of the parameters (temperature and moisture content) in open drying, solar dryer without PCM and with PCM was investigated experimentally. M. Sengar et al., [39], used a mathematical model to investigate drying kinetics and morphological analysis of the dried product. Scanning electron microscopy analysis has been done to examine morphological dried food samples. The study showed a good result / performance because maximum temperatures are reached. The objective of this paper is to study a solar dryer system with a thermal storage bed and humidity absorber. This thermal bed is therefore a porous medium and is placed on the interior facades of the drying chamber. A porous medium is generally composed of a stack of solid particles in which a fluid can flow freely through pores formed between particles. For this, we are interested in materials that are available and less expensive such as basalt and activated carbon. Basalt has a thermal conductivity greater than 1.5W/mk. It is materials that can storage heat for a long time. The principle of drying is to extract the water contained in the product. This will cause high humidity in the drying chamber. To evacuate this humidity we need a material that has pores and micro pores like activated carbon. In Senegal, we have significant basalt resource. Likewise, in Ziguinchor, biomass resources are immense. So it is very easy to obtain biochar to replace activated carbon. The system is experimentally tested using papaya and moringa leaves during the months of February and May 2023 in the climatic conditions of the Ziguinchor region. This is followed by a CFD analysis to better optimize the system.

2. Theoretical Modeling

2.1. Modeling of the Thermal Bed

To simulate the air flow through the thermal bed, we adopted the Darcy-Forchheimer model to describe its behavior as a porous medium. Thus, Darcy showed experimentally that the flow rate of a water flow through a column of sand was proportional to the pressure gradient applied between two sections of this column. The porosity and physical properties of the thermal bed are assumed to be isotopic. Model studied uses of two viscous resistance coefficients $\frac{1}{K}$ and inertial C.

2.2. Governing Equations

In order to optimize the fruit and vegetable drying process in terms of quality, duration and energy efficiency, many researchers are using modeling of this process. The models developed make it possible to simulate the evolution of moisture content, temperature and pressure profiles. The system of equations that governs the convective flow of air through the solar dryer is based on the principles of conservation of mass, momentum and energy. The standard $K-\varepsilon$ model is chosen for the description of turbulent flow. Although there are several other turbulence models, the standard $K-\varepsilon$ model still remains an industrial reference and its applications are found in numerous studies. The equations are written as follows:

2.2.1. Balance Equation at the Air Flow

Continuity equation and momentum equation are given by equations 1, 2 and 3:

$$\frac{\partial u}{\partial x}+\frac{\partial v}{\partial y}=0 \tag{1}$$

$$\rho\left[\frac{\partial u}{\partial t}+\frac{\partial(uu)}{\partial x}+\frac{\partial(vu)}{\partial y}\right]=-\frac{\partial P}{\partial x}+\mu_t\left[\frac{\partial^2 u}{\partial x^2}+\frac{\partial^2 u}{\partial y^2}\right] \tag{2}$$

$$\rho\left[\frac{\partial v}{\partial t}+\frac{\partial(uv)}{\partial x}+\frac{\partial(vv)}{\partial y}\right]=-\frac{\partial P}{\partial x}+\mu_t\left[\frac{\partial^2 v}{\partial x^2}+\frac{\partial^2 v}{\partial y^2}\right]+\rho g\beta(T-T_0) \tag{3}$$

The turbulent kinetic energy k and the dissipation rate ε are written respectively as follow:

$$\rho\left[\frac{\partial k}{\partial t}+\frac{\partial(ku)}{\partial x}+\frac{\partial(kv)}{\partial y}\right]=\left(\mu+\frac{\mu_t}{\sigma_k}\right)\left(\frac{\partial^2 k}{\partial x^2}+\frac{\partial^2 k}{\partial y^2}\right)+G_K-\rho\varepsilon \tag{4}$$

$$\rho\left[\frac{\partial \varepsilon}{\partial t}+\frac{\partial(\varepsilon u)}{\partial x}+\frac{\partial(\varepsilon v)}{\partial y}\right]=\left(\mu+\frac{\mu_t}{\sigma_\varepsilon}\right)\left(\frac{\partial^2 \varepsilon}{\partial x^2}+\frac{\partial^2 \varepsilon}{\partial y^2}\right)+\frac{\varepsilon}{K}(C_1 G_K-C_2\rho\varepsilon) \tag{5}$$

With:

$$\mu_t=\frac{\rho C_\mu K^2}{\varepsilon};\ G_K=\frac{C_\mu}{\rho}\frac{\partial u_i}{\partial x_j}\left[\frac{\partial u_i}{\partial x_j}+\frac{\partial u_i}{\partial x_i}\right]$$

Energy equation is given by equation 6.

$$\rho\left[\frac{\partial T}{\partial t}+\frac{\partial(uT)}{\partial x}+\frac{\partial(vT)}{\partial y}\right]=\left[\frac{\mu}{P_r}+\frac{\mu_t}{\sigma_t}\right]\left[\frac{\partial^2 T}{\partial x^2}+\frac{\partial^2 T}{\partial y^2}\right] \tag{6}$$

2.2.2. Balance Equation on the Racks

To simulate the resistance of the products to be dried to air flow, we modeled the drying racks as a porous medium. Forchheimer proposed an empirical modification of Darcy's law by adding a second-order nonlinear relationship between the pressure gradient and the filtration speed. This formulation is called Darcy-Forchheimer. Porous mediums are modeled with an additional source to the momentum conservation equations given by eq. 7 and eq. 8.

$$\frac{\rho}{\dot{\theta}}\frac{\partial u}{\partial x}+\frac{\rho}{\dot{\theta}^2}\left[u\frac{\partial u}{\partial x}+v\frac{\partial u}{\partial x}\right]=-\frac{\partial P}{\partial x}+\frac{\mu_t}{\dot{\theta}}\left[\frac{\partial^2 u}{\partial x^2}+\frac{\partial^2 u}{\partial y^2}\right]-\mu\frac{u}{K}-\frac{\rho C_F}{\sqrt{K}}|\vec{u}|u \tag{7}$$

$$\frac{\rho}{\dot{\theta}}\frac{\partial v}{\partial x}+\frac{\rho}{\dot{\theta}^2}\left[u\frac{\partial v}{\partial x}+v\frac{\partial v}{\partial x}\right]=-\frac{\partial P}{\partial y}+\frac{\mu_t}{\dot{\theta}}\left[\frac{\partial^2 v}{\partial x^2}+\frac{\partial^2 v}{\partial y^2}\right]-\mu\frac{v}{K}-$$

$$\frac{\rho C_F}{\sqrt{K}}|\vec{v}|v + \rho g\beta(T - T_0) \quad (8)$$

$$K = \frac{D_P^2 \dot{\theta}^3}{150(1-\dot{\theta})^2} \quad (9)$$

$$C_F = \frac{3{,}5(1-\dot{\theta})}{D_P \dot{\theta}^3} \quad (10)$$

Another flow model in porous media was proposed by introducing the source term by expressing the pressure gradient as a power law of the velocity amplitude:

$$S_i = -C_0|v|^{C_L} \quad (11)$$

The solid phase and the air in the pores are assumed to be in thermal equilibrium. Thus, the energy conservation is given by:

$$(\rho C_P)_m \frac{\partial T}{\partial t} + (\rho C_P)_m \left(u_f \frac{\partial T}{\partial x} + v_f \frac{\partial T}{\partial y}\right) = \lambda_m \frac{\partial}{\partial x}\left(\frac{\partial^2 T}{\partial x^2} + \frac{\partial^2 T}{\partial x^2}\right) \quad (12)$$

Porous medium density, heat capacity and thermal conductivity are calculated as follows:

$$(\rho C_P)_m = \dot{\theta}(\rho C_P)_f + (1 - \dot{\theta})(\rho C_P)_S \quad (13)$$

$$\lambda_m = \dot{\theta}\lambda_f + (1 - \dot{\theta})\lambda_S \quad (14)$$

3. Measurement and Experimentation Equipment

The solar dryer is composed of a flat glass collector (100×50 cm) and a drying chamber (100 cm x 80 cm x 60 cm). The two are connected by a pipe as shown in figure 1 and a photovoltaic system associated with a battery for operating the fans. The sensor is placed on a support equipped with a crank allowing the inclination angle of the sensor to be varied between 0 and 90 °. Two fans with a power of 12V are placed at the inlet of the solar plate collector to increase the air flow and ensure its renewal in the drying chamber. With the temperature gradient, the air heated by the solar flat collector passes through the pipe and reaches the drying racks in order to dry the food product. The interior of the drying chamber is made of galvanized sheet metal and contains 4 drying racks whose contours are made of aluminum. The drying chamber is in the form of a cone with an inverted top. It is connected to the heated air coming into the solar flat collector by pipe. It serves to dissipate heat to all corners of the drying chamber. This is the part where the thermal bed used for heat storage and humidity absorber will be lined. The thermal bed is placed below the four racks as shown in figure 2. The air heated by the solar flat collector first flows towards the thermal bed and heats the gravel before reaching the drying racks and the product to be dried. This phenomenon ensures improvement in the natural draw of drying air in the chamber. The other part of heat is stored in thermal bed to compensate for the deficit during non-sunny hours.

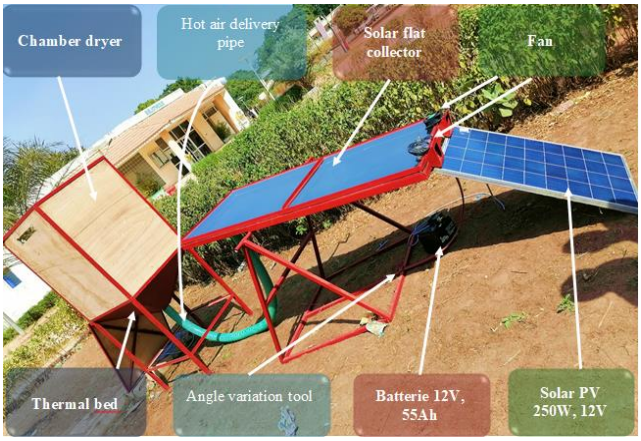

Figure 1. *View of the solar dryer studied.*

Figure 2. *Thermal bed inside the solar dryer.*

The drying and control of the various products were carried out using an electronic balance with a capacity of 410 g and a precision equal to 0.001 g, thermocouples for temperature measurement in different levels of the drying chamber, the thermal bed, the solar flat collector, and the ambient air. We have also two fans of 12V capacity placed at the inlet of the solar flat collector to vary the air flow in the drying chamber, a photovoltaic kit associated with a battery for the fan operation. Moringa leaves and papaya are used as drying products. Figure 3a and figure 3b gives the papaya and moringa oleifera dryed in the chamber dryer.

a b

Figure 3. *a. Papaya drying; b. Moringa oleifera leaves drying.*

4. Results and Discussions

4.1. Experimental Results

The results obtained are presented by highlighting the influence of the thermal bed on the behavior of the dryer. They are obtained by taking into account the experimental conditions, namely temperature, humidity and air velocity.

Figure 4 and figure 5 give the temperatures of thermal bed, ambient environment, the air at the inlet of dryer chamber, the air at the dryer outlet as a function of time during the drying of papaya slices.

The experiment duration took place in two days with an average ambient temperature of 32.67 ℃. The following analysis reveals an average temperature variation for the two days of drying the papaya. At 10:00 a.m. to 2:00 p.m., temperature variations were noted at the level of the thermal bed, the air between the drying racks and the air at the outlet of the drying chamber, respectively an average of 40 ℃, 39, 33 ℃ and 37.89 ℃. An intermediate phase is noted. It started from 2:00 p.m. to 6:00 p.m. with an average ambient temperature of 33.89 ℃. The temperatures at the level of the thermal bed, the air between the drying racks and the air at the outlet of the drying chamber are respectively 46.44 ℃, 45.33 ℃ and 43.78 ℃. A final phase from 6:00 p.m. to 10:00 p.m. provides an overview of the heat storage by the thermal bed. Thus, the temperatures at the level of the thermal bed, the air between the drying racks and the air at the outlet of the drying chamber are respectively an average of 48.67 ℃, 48 ℃ and 47.22 ℃, compared to 34.33 ℃ of the ambient temperature, a difference of more than 4 ℃. This is due to the fact that the increase in the density of the incident solar flux in the morning, the thermal bed stores a large quantity in order to release it to compensate for the intermittency of the sun.

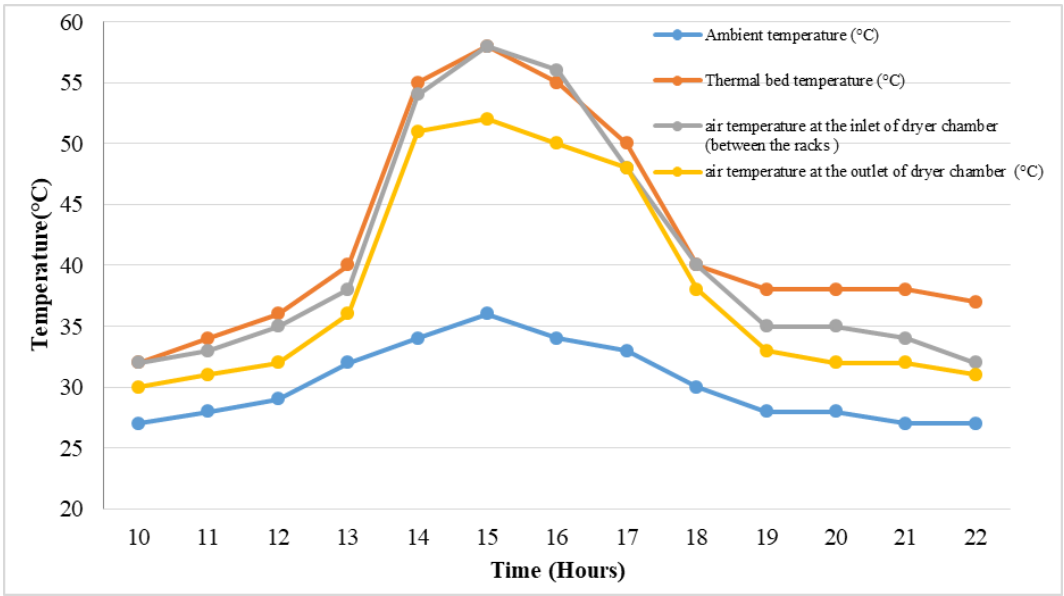

Figure 4. *Temperature variations in the drying chamber on the first day for papaya slices (13/02/2023).*

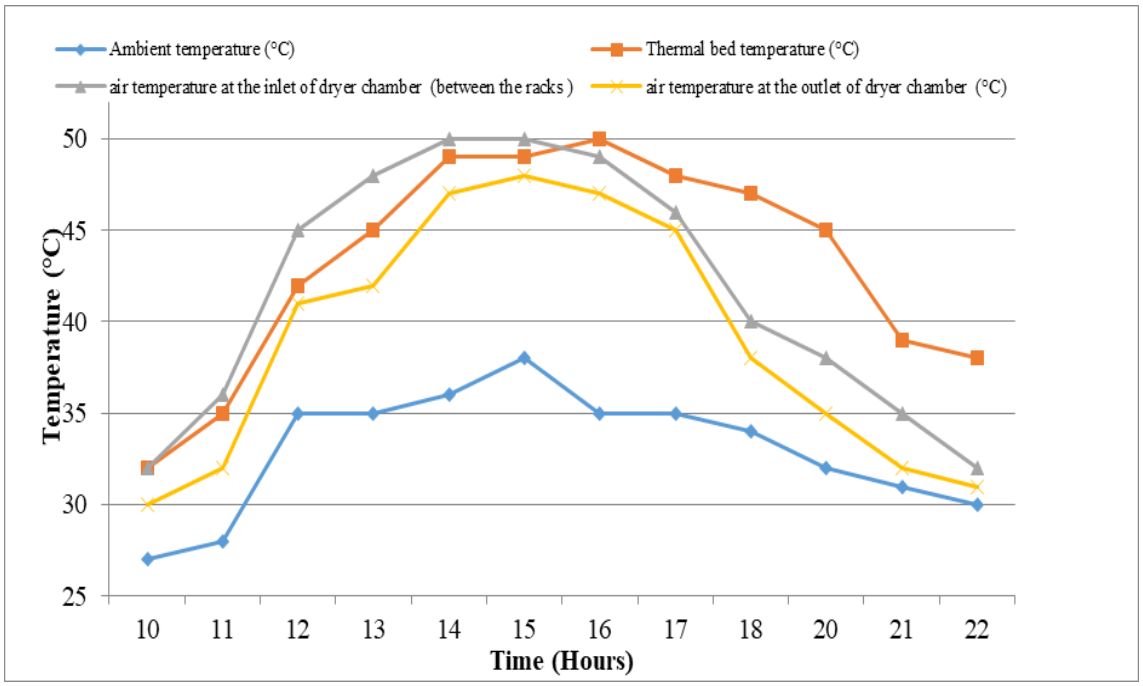

Figure 5. *Temperature variations in the drying chamber on the second day for papaya slices (14/02/2023).*

Figure 6 gives the temperatures of the thermal bed, the ambient environment, the air at the solar flat collector outlet, the air at the dryer outlet as a function of time during the drying of moringa's leaves.

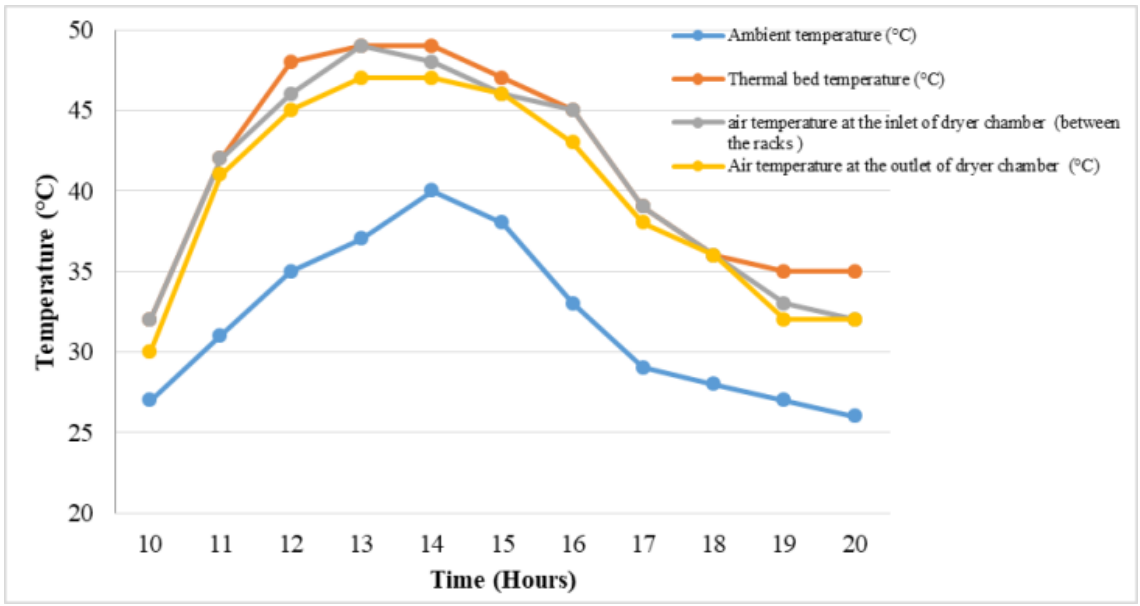

Figure 6. *Temperature variations in the drying chamber on the first day for moringa's leaves (17/02/2023).*

The results obtained during the experiments show that the temperature is not uniform inside the dryer. However, it is imperative to point out that the temperature of the moringa leaves should not exceed 55 ℃ as shown in figure 6 to avoid their deterioration. Drying takes place in one day. For an ambient temperature of 37.33 ℃, the temperatures at the thermal bed, the air between the drying racks and the air at the outlet of the drying chamber are respectively 48.67 ℃; 47.67 ℃ and 46.33 ℃.

Dried products dehydrate by releasing water. The hot air in the drying chamber becomes humid. This humidity will have a negative impact on the quality of the product.

Figure 7 and figure 8 show the evolution of water content of papaya slices.

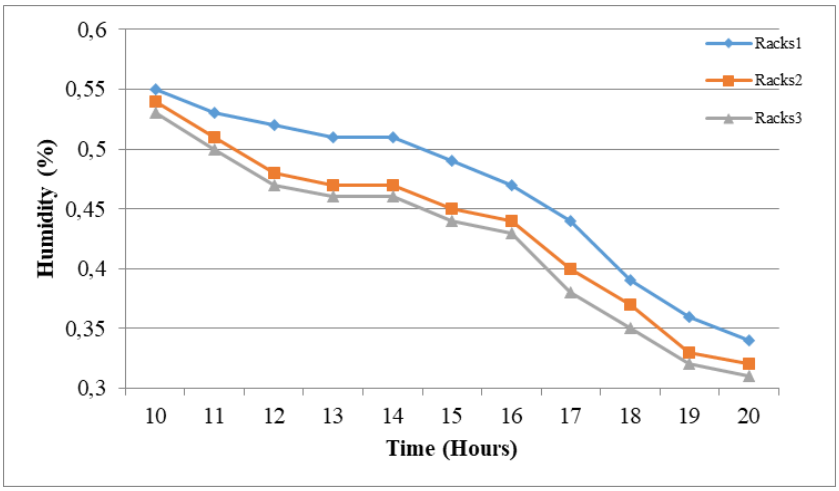

Figure 7. *Variation in water content of papaya for the first day of drying (13/02/2023).*

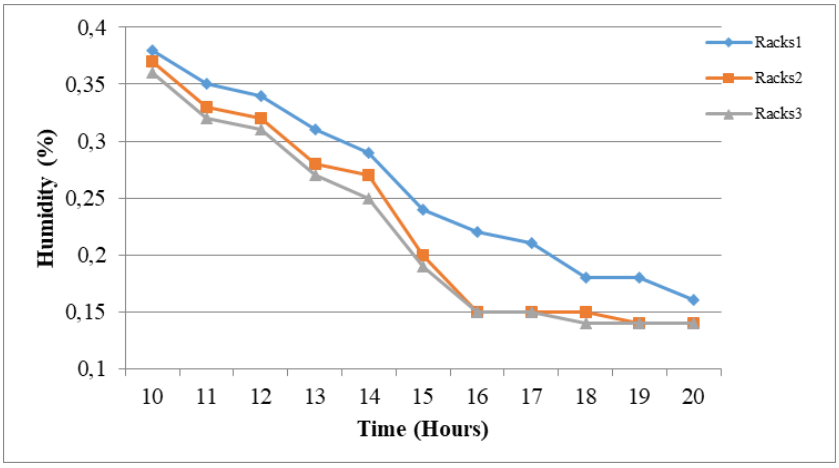

Figure 8. *Variation in water content of papaya slices on the second day of drying (14/02/2023).*

Figure 7 and figure 8 show decreasing curves of papaya water content. Figure 8 shows that on the second day of drying, the water content is 15% and was reached at the level of the three racks.

Figure 9 shows the evolution of the water content of moringa leaves.

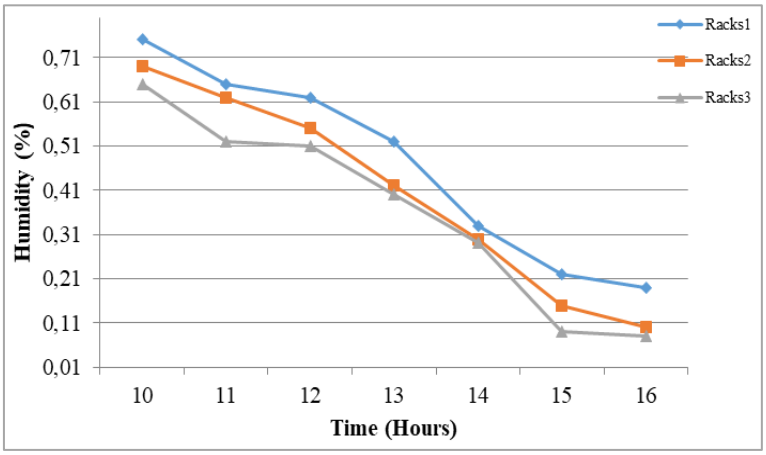

Figure 9. *Variation in water content of moringa leaves (17/02/2023).*

Figure 9 shows that the humidity level of the moringa leaves varies for the rack 1, 2 and 3, respectively from 75% to 19%; from 69% to 8%; and from 65% to 8%.

4.2. Numerical Results

In a proactive approach to embracing technological advancements, our study integrates Computational Fluid Dynamics (CFD) to enhance the sophistication of our investigation into food drying processes. Using the state-of-the-art Ansys Fluent software, we meticulously simulate the solar dryer system by incorporating precise geographical coordinates for Ziguinchor's region (latitude: 12.5565°N, longitude: 16.2719°W). Our approach ensures a high level of accuracy by considering the region's solar flux, climate conditions, and time zone (UTC). This commitment to precision enhances the reliability and relevance of our CFD analysis, contributing to a comprehensive understanding of the system's behavior. This methodology aligns with previous research emphasizing the importance of integrating CFD in modeling solar dryers. Figures 10 to 16 give the CFD simulation results.

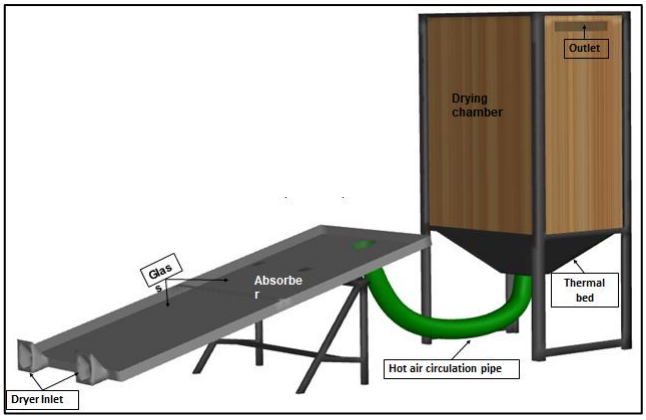

Figure 10. *3D simulation geometry of the dryer.*

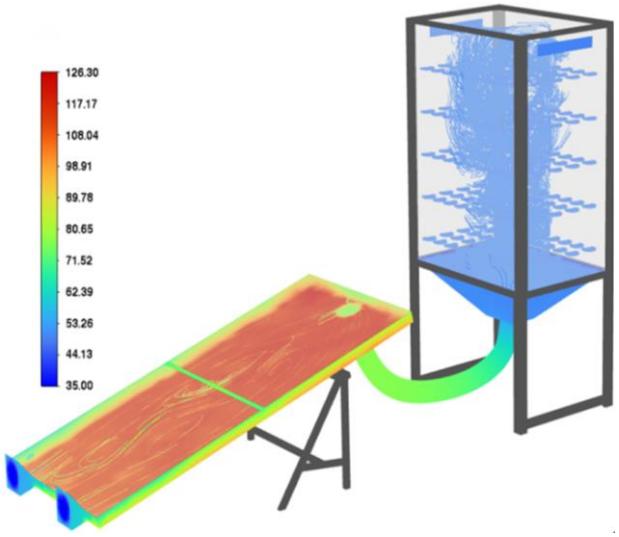

Figure 11. *Temperature evolution in the solar plat collector.*

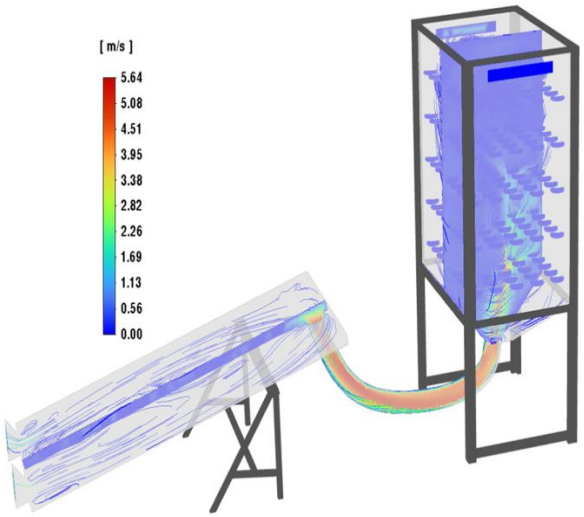

Figure 12. *Velocity evolution in the dryer.*

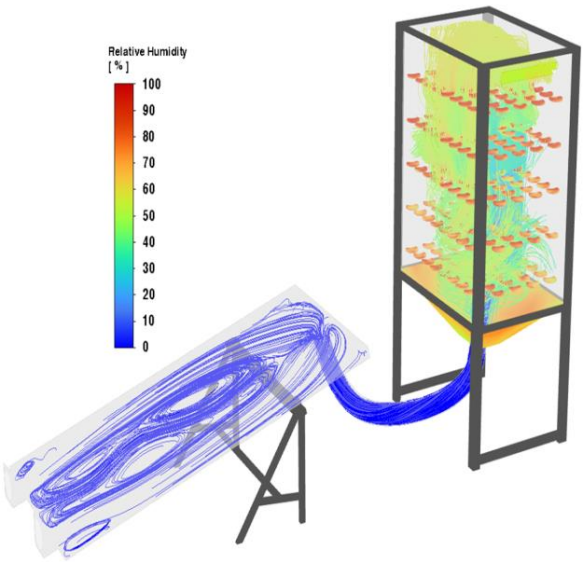

Figure 13. *Humidity evolution in the dryer chamber.*

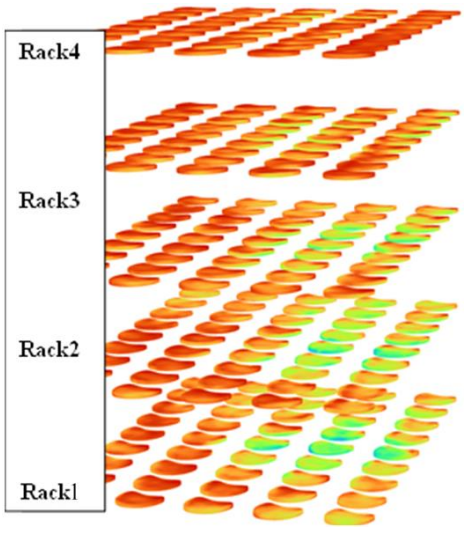

Figure 14. *Dryer product on the racks.*

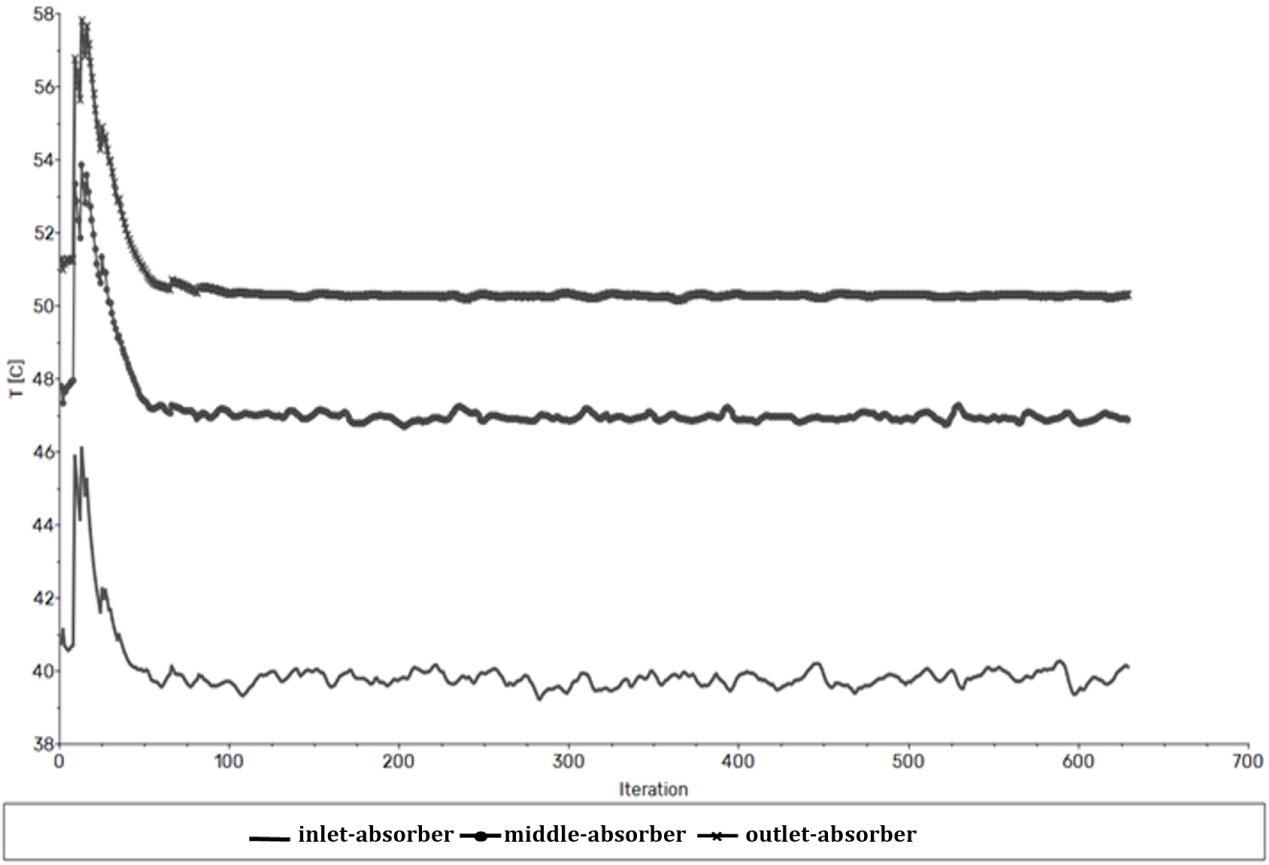

Figure 15. *Temperature evolution inside absorber of solar plat collector.*

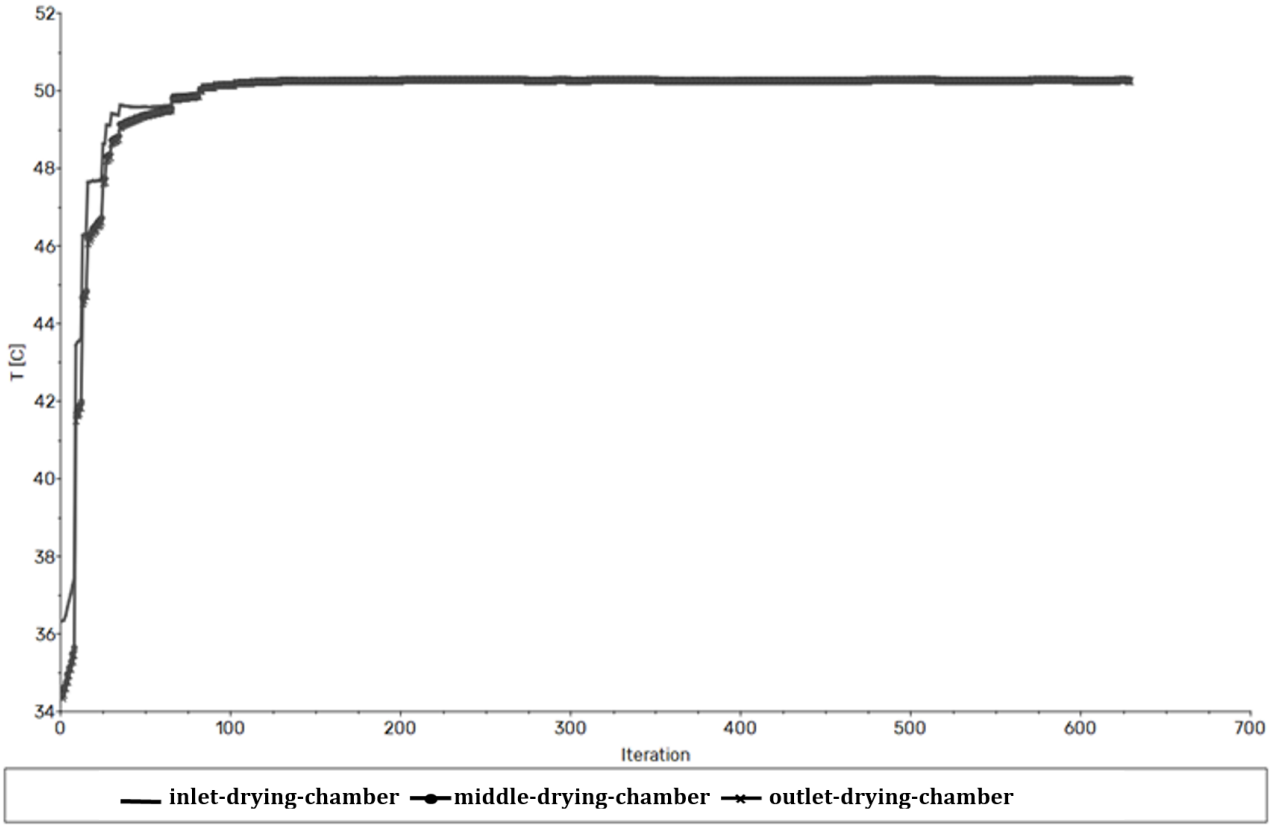

Figure 16. *Temperature evolution inside the dryer chamber.*

Figure 10 gives the three (3D) simulation geometry of the study system. Figure 11 and figure 12 illustrate the evolution of temperature within the solar flat collector and the velocity of hot air within the dryer, respectively. Figure 13 and figure 14 depict the humidity levels within the dryer. Notably, to better understand temperature dynamics within the dryer, we positioned points corresponding to the experimental temperature probes at the entrance, middle, and exit of both the absorber and the drying chamber as it is shown in Figures 15 and 16. Resulting temperature profiles accurately depict variations within the dryer with maximum temperature of 50 ℃ in the drying chamber at the third time of the experiment. As air moves through the absorber, temperature fluctuations decrease, attributed to a uniform and stable flow regime that equalizes temperatures throughout the dryer. These simulation results validate the experimental model and provide deeper insights into the dynamics of the drying process. This study aims to observe the behavior of the thermal bed integrated into the drying chamber. To conduct the experiments, slices of papaya and moringa leaves were utilized, as shown in Figure 3a and figure 3b. The results indicated that the thermal bed could retain heat until 10 p.m. with a temperature of 39 ℃. Experimental findings demonstrated that the maximum moisture content of papaya which is (15%) was achieved within three days of drying, while moringa leaves (8%) reached the desired moisture level within two days. The ability of the thermal bed to store and slowly release heat is crucial for maintaining optimal drying conditions even after sunset. The CFD results showed the temperature evolution within the solar collector and drying chamber, as well as changes in humidity and the velocity of hot air within the dryer. The CFD model provides a detailed analysis of the heat and mass transfer processes occurring within the dryer, enabling the identification of key parameters that influence drying efficiency. This advanced modeling approach will facilitate the optimization of solar dryer designs, enhancing their performance and sustainability. Our research underscores the effectiveness of combining experimental data with advanced simulation tools such as CFD to improve the design and operation of solar drying systems. The integration of CFD in our study not only validates the experimental findings but also provides a robust framework for future investigations aimed at optimizing solar dryer performance under various climatic conditions. This comprehensive approach is essential for developing efficient and sustainable food preservation technologies that can be widely adopted in regions with abundant solar resources.

5. Conclusion

The objective of this paper is to analyze the behavior of thermal bed integrated into the drying chamber of the dryer. To conduct this experiment, papaya slices and moringa leaves were used. The results showed that the thermal bed could store heat until 10 p.m., maintaining a temperature of 39 ℃. The experiments revealed that the final moisture content of 15% for papaya is achieved in three days of drying, while that of 8% for moringa leaves is reached in two days of drying. To optimize the performance of our dryer, a CFD simulation was conducted using Ansys Fluent to validate the experiment. This simulation allowed for the optimization of dryer characteristics, such as glass thickness, the optimal air velocity at the inlet of the absorption chamber, and the spacing of the drying racks. It also enabled the visualization of temperature evolution in the solar collector and drying chamber. Furthermore, it demonstrated humidity evolution and hot air velocity in the collector, as well as heat dissipation in the dryer, which closely matched the experimental study results. In the future, it would be important to conduct a comparative optimization study using CFD on the thermal and hygrometric behavior of a thermal bed made of basalt and biochar, respectively serving as heat storage and moisture absorber.

Abbrevation

K	Turbulent Kinetic Energy, m^2s^{-2}
ε	Dissipation of Turbulent Kinetic Energy, m^2s^{-3}
ρ	Density, $kg.m^{-3}$
μ	Viscosity, Pa.s
μ_t	Turbulent Dynamic Viscosity, $Kg.m^{-1}s^{-1}$
C_μ	Turbulence Model Constants
$u,\ v$	Velocity, $m.s^{-1}$
P	Pressure, Bar
C_P	Constant Pressure Specific Heat, $kJ.kg^{-1}K^{-1}$
C_F	Inertial Resistance Factor
T	Temperature, K
C_F	Inertial Resistance Factor, m^{-1}
D_P	Particle Diameter, m
g	Gravitational Acceleration, $m.s^{-2}$
λ	Thermal Conductivity, $W.m^{-1}K^{-1}$
G_K	Turbulence Model Constant $K-\varepsilon$
S_i	Source Term
$\sigma_t,\ \sigma_k,\ \sigma_\varepsilon$	Constants Involved in the Model $K-\varepsilon$
$C_0,\ C_1, C_2\ C_L$	Empirically Coefficients
$\dot{\theta}$	Porosity
P_r	Prandtl Number
β	Coefficient of Expansion
S	Solid Phase in the Thermal Bed
f	Fluid Phase in the Thermal Bed
m	Blend

Author Contributions

Serigne Thiao: Conceptualization, Funding acquisition,

Investigation, Methodology, Project administration, Resources, Validation, Writing – original draft

Omar Drame: Data curation, Funding acquisition, Investigation, Resources, Software

Awa Mar: Funding acquisition, Investigation, Project administration, Resources

Lat Grand Ndiaye: Methodology, Resources, Supervision, Validation

Issakha Youm: Formal Analysis, Resources, Supervision, Validation

Acknowledgments

This work was supported by the laboratory of chemistry and physics of materials of the Assanse Seck University of Ziguinchor, Senegal.

Conflicts of Interest

The authors declare no conflicts of interest.

References

[1] Cliquet, R. and Thienpont, K. (1995). Population and Development: a Message from The Cairo Conference. London: Kluwer Academic Publishers) ISBN: 0792337638 (alkaline paper) (hardback).

[2] Dyson, T. (1996). Population and Food: Global Trends and Future Prospects. Global Environmental Change Series. London: Routledge. 231 p.). Library of Congress Cataloguing in Publication Data, ISBN 0-203-97715-7 Master e-book ISBN.

[3] A. Dwivedi et al., (2023) Prioritization of potential barriers to the implementation of solar drying techniques using MCDM tools: A case study and mapping in INDIA, Solar Energy 253, 199–218, https://doi.org/10.1016/j.solener.2023.02.030

[4] B. V. Suresh et al., (2023) Natural energy materials and storage systems for solar dryers: State of the art, Solar Energy Materials and Solar Cells 255, 112276, https://doi.org/10.1016/j.solmat.2023.112276

[5] V. R. Mugi et al., (2022) A review of natural energy storage materials used in solar dryers for food drying applications, Journal of Energy Storage 49, 104198, https://doi.org/10.1016/j.est.2022.104198

[6] G. N. Abdel-Rahman et al., (2023) Safety improvement of the open sun dried Egyptian Siwi dates using closed solar dryer, Heliyon 9, e22425, https://doi.org/10.1016/j.heliyon.2023.e22425

[7] M. C. Ndukwu et al., (2023) Progressive review of solar drying studies of agricultural products with exergoeconomics and econo-market participation aspect, Cleaner Environmental Systems 9. 100120, https://doi.org/10.1016/j.cesys.2023.100120

[8] E. G. Barbosa et al., (2023) Thermal energy storage systems applied to solar dryers: Classification, performance, and numerical modeling: An updated review, Case Studies in Thermal Engineering 45, 102986, https://doi.org/10.1016/j.csite.2023.102986

[9] H. S. EL-Mesery et al., (2022) Recent developments in solar drying technology of food and agricultural products: A review, Renewable and Sustainable Energy Reviews 157, 112070, https://doi.org/10.1016/j.rser.2021.112070

[10] T. Kreetachat et al., (2023) Dataset on the optimization by response surface methodology for dried banana products using greenhouse solar drying inThailand, Data in Brief 49, 109370. https://doi.org/10.1016/j.dib.2023.109370

[11] H. M. Denise et al., (2023) Solar drying modes of saladette tomatoes slices on phytochemicals and functional properties, Solar Energy 262, 111903, https://doi.org/10.1016/j.solener.2023.111903

[12] M. Usama et al., (2023) The energy, emissions, and drying kinetics of three-stage solar, microwave and desiccant absorption drying of potato slices, Renewable Energy 219, 119509, https://doi.org/10.1016/j.renene.2023.119509

[13] C. Prajapati and T. Sheorey, (2023) Exploring the efficacy of natural convection in a cabinet type solar dryer for drying gooseberries: An experimental analysis, Journal of Agriculture and Food Research 14, 100684, https://doi.org/10.1016/j.jafr.2023.100684

[14] R. J. Mongi, (2023) Physicochemical properties, microbial loads and shelf life prediction of solar dried mango (Mangifera indica) and pineapple (Ananas comosus) in Tanzania, Journal of Agriculture and Food Research 11, 100522, https://doi.org/10.1016/j.jafr.2023.100522

[15] M. Emamjome Kashan et al., (2023) Insulated concrete form foundation wall as solar thermal energy storage for Cold-Climate building heating system, Energy Conversion and Management: X 19, 100391, Energy Conversion and Management: X 19 (2023) 100391.). https://doi.org/10.1016/j.ecmx.2023.100391

[16] A. Arefian et al., (2024) A comprehensiveanalysis of time-dependent performance of a solar chimney power plant equipped with a thermal energy storage system, Renewable and Sustainable Energy Reviews 189, 114051, https://doi.org/10.1016/j.rser.2023.114051

[17] C. Zhou et al., (2023) Simulation and economic analysis of an innovative indoor solar cooking system with energy storage, Solar Energy 263, 111816, https://doi.org/10.1016/j.solener.2023.111816

[18] A. Hassan et al., (2023) Transient analysis and techno-economic assessment of thermal energy storage integrated with solar air heater for energy management in drying, Solar Energy 264, 112043, https://doi.org/10.1016/j.solener.2023.112043

[19] J. Ellis et al., (2023) Solar crop dryer with thermal energy storage as backup heater, Solar Compass 8, 100058, https://doi.org/10.1016/j.solcom.2023.100058

[20] T.-C. Ong et al., (2024) Review on the challenges of salt phase change materials for energy storage in concentrated solar power facilities, Applied Thermal Engineering 238, 122034, Applied Thermal Engineering 238 (2024) 122034.) https://doi.org/10.1016/j.applthermaleng.2023.122034

[21] A. Svobodova-Sedlackova et al., (2024) Thermal stability and durability of solar salt-based nanofluids in concentrated solar power thermal energy storage: An approach from the effect of diverse metal alloys corrosion, Journal of Energy Storage 75, 109715, https://doi.org/10.1016/j.est.2023.109715

[22] Serigne, T, Omar, D, Awa, M, Lat Grand, N, Issakha, Y. Experimental and Numerical CFD Analysis of A Solar Dryer with Integration of Basalt Thermal Bed for Heat Storage. 12. Eur. Conf. Ren. Energy Sys. 16-17 May 2024, Mallorca, Spain.

[23] U. Pelay, L. Luo, Y. Fan, D. Stitou, M. Rood, (2017) Thermal energy storage systems for concentrated solar power plants, Renew. Sustain. Energy Rev. 79, 82–100, https://doi.org/10.1016/j.rser.2017.03.139

[24] A. Palacios, C. Barreneche, M. E. Navarro, Y. Ding, (2020) Thermal energy storage technologies for concentrated solar power – a review from a materials perspective, Renew. Energy 156, 1244–1265, https://doi.org/10.1016/j.renene.2019.10.127

[25] M. Barnetche et al., (2023) Optimum integration of latent heat storage in a solar thermal system for industrial processes: In series or in parallel?, Applied Thermal Engineering 232, 121090, https://doi.org/10.1016/j.applthermaleng.2023.121090

[26] N. Divyangkumar, S. Jain and N. L. Panwar, (2022) Influences of latent heat storage heat sink integrated with solar dryer to enhance drying period, Energy Nexus 8, 100160, https://doi.org/10.1016/j.nexus.2022.100160

[27] Y. Muhammad et al., (2023) Rock bedthermal energy storage coupled with solar thermal collectors in an industrial application: Simulation, experimental and parametric analysis, Journal of Energy Storage 67, 107349, https://doi.org/10.1016/j.est.2023.107349

[28] M. C. Gilago, V. R. Mugi and C. V. P., (2023) Performance assessment of passive indirect solar dryer comparing without and with heat storage unit by investigating the drying kinetics of carrot, Energy Nexus 9, 100178, https://doi.org/10.1016/j.nexus.2023.100178

[29] D. Tadele Embiale and D. Gudeta Gunjo, (2023) Investigation on solar drying system with double pass solar air heater coupled with paraffin wax based latent heat storage: Experimental and numerical study, Results in Engineering 20, 101561, https://doi.org/10.1016/j.rineng.2023.101561

[30] H. U. Rehman et al., (2023) An experimental case study of solar food dryer with thermal storage using phase change material, Case Studies in Thermal Engineering 51, 103611, https://doi.org/10.1016/j.csite.2023.103611

[31] Majeed, A. H., Faraj, J. J., Hussien, F. M. (2024). Enhancing solar drying efficiency through indirect solar dryers integrated with phase change materials. International Journal of Heat and Technology, Vol. 42, No. 1, pp. 121-131. https://doi.org/10.18280/ijht.420113

[32] Jaworski, M., Rusowicz, A., Grzebielec, A., & Szelągowski, A. (2023). Experimental Investigation of PCM Based Thermal Energy Storage Unit with Finned Tubes. In *11. EUROPEAN CONFERENCE on RENEWABLE ENERGY SYSTEMS*. Turchia., 2023.

[33] Thaker, A. S., Hussien, F. M., Faraj, J. J. (2023). Numerical simulation of an indirect solar dryer equipped with thermal conduction enhancer augmented phase change materials (PCMs) for banana drying. International Journal of Heat and Technology, Vol. 41, No. 5, pp. 1158-1166. https://doi.org/10.18280/ijht.410506

[34] S. Madhankumar et al., (2023) A review on the latest developments in solar dryer technologies for food drying process, Sustainable Energy Technologies and Assessments 58, 103298, https://doi.org/10.1016/j.seta.2023.103298

[35] P. Lad et al., (2023) Numerical investigationof phase change material assisted indirect solar dryer for food quality preservation, International Journal of Thermofluids 18, 100305, https://doi.org/10.1016/j.ijft.2023.100305

[36] S. e.-D. Fertahi et al., (2023) CFD Investigation of Fin Design Influence on Phase Change Material Melting for Solar Thermal Energy Storage, e-Prime - Advances in Electrical Engineering, Electronics and Energy 6, 100306, https://doi.org/10.1016/j.prime.2023.100306

[37] Petros Demissie et al., (2019) Design, development and CFD modeling of indirect solar food dryer, Energy Procedia 158, 1128–1134, http://creativecommons.org/licenses/by-nc-nd/4.0/

[38] S. Rakshamuthu et al., (2021) Experimental analysis of small size solar dryer with phase change materials for food preservation, Journal of Energy Storage 33, 102095, https://doi.org/10.1016/j.est.2020.102095

[39] M. Sengar et al., (2023) Drying kinetics, thermal and morphological analysis of starchy food material: Experimental investigation through an induced type solar dryer, Environmental Technology & Innovation 31, 103221, https://doi.org/10.1016/j.eti.2023.103221